Theoretical Modeling of Oscillation Characteristics of Oscillating Capillary Tube Heat Pipe

Ngoc Hung Bui, Jong-Soo Kim*†, Hyun-Seok Jung**

Graduate Student, Refrigeration and Air-Conditioning Eng., Pukyong National University, Busan 608-737, Korea

**School of Mechanical Eng., Pukyong National University, Busan 608-737, Korea*

***Samsung Electronics Co. Ltd., Kyungki-Do 442-742, Korea*

Key word: Oscillating capillary tube heat pipe (OCHP), Theoretical modeling

ABSTRACT: The examinations of the operating mechanism of an oscillating capillary tube heat pipe (OCHP) using the visualization method revealed that the working fluid in the OCHP oscillated to the axial direction by the contraction and expansion of vapor plugs. The contraction and expansion were due to the formation and extinction of bubbles in the evaporating and condensing part, respectively. The actual physical mechanism, whereby the heat which was transferred in such an OCHP was complex and not well understood. In this study, a theoretical model of the OCHP was developed to model the oscillating motion of working fluid in the OCHP. The differential equations of two-phase flow were applied and simultaneous non-linear partial differential equations were solved. From the analysis of the numerical results, it was found that the oscillating motion of working fluid in the OCHP was affected by the operation and design conditions such as the heat flux, the charging ratio of working fluid and the hydraulic diameter of flow channel. The simulation results showed that the proposed model and solution could be used for estimating the operating mechanism in the OCHP.

Nomenclature

d : inner hydraulic diameter [m]
f : friction factor
F : frictional force per unit volume [N/m^3]
g : gravitational acceleration [m/s^2]
G : mass velocity [kg/m^{2}s]
h : specific enthalpy [J/kg]
L : length [m]
p : pressure [Pa]
q : heat flux [W/cm^2]
t : time [s]
u : axial velocity [m/s]
v : specific volume [m^3/kg]
x : axial coordinate [m]
X : vapor quality
X_{tt} : martinelli parameter

Greek symbols

α : charging ratio [%]
μ : dynamic viscosity [kg/ms]
υ : kinematic viscosity [m^2/s]
ρ : density [kg/m^3]
τ : shear stress [N/m^2]

Subscripts

f : saturated fluid
fg : saturated vapor-fluid
g : saturated vapor

† Corresponding author
Tel.: +82-51-620-1502; fax: +82-51-611-6368
E-mail address: jskim@pknu.ac.kr

w : wall

1. Introduction

The oscillating capillary tube heat pipe (OCHP) is a very promising heat transfer device.[1] In addition to its excellent heat transfer performance, it has a simple structure: in contrast with conventional heat pipes, there is no wick structure to return the condensed working fluid back to the evaporating part. The OCHP is made from a long continuous capillary tube bent into many turns of serpentine structure. The working fluid is charged into the OCHP. The diameter of the OCHP must be sufficiently small so that vapor plugs can be formed by capillary action. The OCHP is operated within a 0.1~5 mm inner diameter range. The OCHP can operate successfully for all heating modes. The heat input, which is the driving force, increases the pressure of the vapor plugs in the evaporating part. In turn, this pressure increase will push neighboring vapor plugs and liquid slugs toward the condensing part, which is at a lower pressure. However, due to the continuous heating, small bubbles formed by nucleate boiling. The bubbles grow and coalesce to become vapor plugs. The flow of the vapor plugs and liquid slugs moves to the condensing part by pressure difference. The heat transfer continuously occurs. As a result, thermal energy is rapidly transferred from the evaporating part to the condensing part as well as the oscillation and circulation of liquid slugs and vapor plugs occurring in the OCHP.[2]

Both experimental and numerical investigations on OCHP have been carried out by some researchers. The experiments mainly focus on the visualization of flow pattern and the measurement of temperature and effective thermal conductivity. While most researchers suggest that slug flow is the dominate flow pattern, Kim et al.[3] and Lee et al.[4] reported that the oscillation of vapor bubbles caused by nucleate boiling and vapor oscillation and the departure of small bubbles are considered as the representative flow patterns at the evaporating part and at the adiabatic part, respectively. The available experimental data can provide some base for verification of the theoretical model. To predict the oscillatory flow characteristics, Miyazaki and Arikawa[5] proposed a theoretical model, which was strongly supported by experimental results. The visualization test showed that the oscillatory flow formed waves that traveled among the turns of the oscillating heat pipes. Their theoretical model could be used to estimate the pressure and displacement of oscillatory flow.

Dobson and Harms[6] performed a lumped parameter analysis on oscillatory heat pipes. The mathematical model is given for a heat pipe with an open end, and they mentioned that it can be applied also to the heat pipe with a closed end. They assumed that the effect of surface tension is negligible. They also assumed that there is no heat transfer between the liquid and its surroundings. The heat transfer coefficient between heated pipe wall and the vapor was simply assumed.

Wong et al.[7] presented a theoretical modeling of the pulsating heat pipe. The liquid film between the vapor plug and the wall is neglected, and the effect of surface tension was not taken into account. The capillary heat pipe is modeled under adiabatic conditions and there is no heat input at any part of the heat pipe. The local heat input is simulated as a sudden pressure pulse applied to a vapor plug at the evaporating part. Despite these over-simplifications, the propagation of pressure wave in the capillary heat pipe is successfully modeled.

There have been experimental studies, which proposed the existence of chaos in OCHPs under some operating conditions.[8,9] The approach in these studies was to analyze the time series of fluctuation of temperature of a specified location on the OCHP tube wall (adiabatic part) by

power spectrum calculated through Fast Fourier Transform. The two dimensional mapping of the strange attractor and the subsequent calculation of the Lyapunov exponent have been done to prove the existence of chaos in the OCHP. A theoretical study on the most single loop of the OCHP has also been undertaken.[10] In their study, basic equations of two-phase flow were applied and it was concluded that chaotic dynamics governs the flow over a wide range of heat transfer rates.

This study introduces a theoretical model of a closed loop of OCHP. The OCHP has been simplified into two turns including three parts: evaporating, condensing and adiabatic part that covers the real application form of the OCHP. The friction factor of the two-phase flow has been evaluated by applying a suitably defined single-phase friction factor to two-phase flow. The differential equations of a two-phase flow were applied and simultaneous non-linear partial differential equations were solved. The variations of mass velocity with respect to time was calculated based on the changes of the operation and design conditions such as the heat flux, the charging ratio of working fluid and the hydraulic diameter of flow channel.

2. Theoretical model of OCHP

2.1 Principle theory

Figure 1 illustrates a schematic of OCHP with serpentine channel that was partially filled with a working fluid. As heating is applied to the evaporating part and cooling is applied to the condensing part of the OCHP. Vapor bubbles generate in the evaporating part and condense into liquid slugs in the condensing part. The volume expansion due to the vaporization and contraction due to the condensation cause an oscillating motion of the working fluid that propels vapor plugs (carrying heat) toward the condensing part and returns liquid to the evaporating part. The oscillatory motion of the liquid slugs and vapor plugs is self-sustained as long as the heating and cooling conditions are maintained.

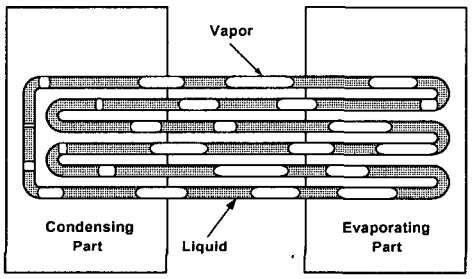

Fig. 1 Schematic of oscillating capillary tube heat pipe.

2.2 Governing equations

The theoretical model of the OCHP, studied in this paper, is illustrated in Fig. 2. It is an OCHP that has been simplified into two turns.

The following assumptions are made in developing the simplified form of the governing equations.

(1) The phases of the working fluid are in thermo-dynamic equilibrium.

(2) Flow model is homogeneous and there is a no-slip flow.

(3) Flow model is a one-dimensional model.

(4) Contribution of the kinetic and pressure energy terms in the energy equation is small

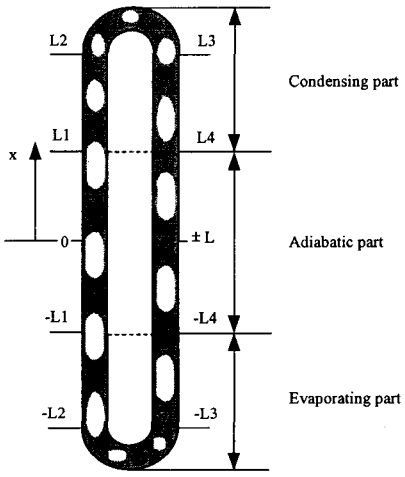

Fig. 2 Model of a single loop of the OCHP.

compared to the enthalpy of the fluid and the heat transfer rates.

Depending on the above assumptions, the governing equations for the different parts of the OCHP can be written as follows.

- Momentum equation

Using the relation, $G=\rho u$, the momentum equation may be written as:

$$\frac{\partial G}{\partial t}+\frac{\partial}{\partial x}\left(\frac{G^2}{\rho}\right)=-\frac{\partial p}{\partial x}-F\pm\rho g \qquad (1)$$

where, the first term on the right side of Eq. (1) gives the total static pressure gradient as evaluated from the homogeneous model, the second term gives the total wall shear force per unit volume of pipe and the third term is the effect of the gravity force.

- Energy equation

The energy equation can be expressed in terms of the enthalpy and mass velocity as:

$$\rho\frac{\partial h}{\partial t}+G\frac{\partial h}{\partial x}=\pm\frac{4}{d_h}q \qquad (2)$$

where, h is the specific enthalpy of the homogeneous fluid and the right side of Eq. (2) represents the heat transfer rate between the pipe wall and working fluid.

3. Solution

Assuming that the heat inputted to the evaporating part and the heat rejected from the condensing part is constant, q_0. The heat flux, q, is expressed in the following form

$$q=f(x)=\begin{cases} q_0(-L_4\le x\le -L_1) \\ 0(-L_1<x<L_1) \\ 0(L_4<x\le L) \\ 0(-L\le x<-L_4) \\ -q_0(L_1\le x\le L_4) \end{cases} \qquad (3)$$

Approximating the above Eq. (3) to the Fourier series on displacement $[-L\sim L]$

$$f(x)=\frac{a_0}{2}+\sum_{n=1}^{\infty}\left[a_n\cos\left(\frac{n\pi x}{L}\right)+b_n\sin\left(\frac{n\pi x}{L}\right)\right] \qquad (4)$$

where a_n, b_n, are the Fourier series coefficients. Because $f(x)$ is "odd function", Eq. (4) can be expressed in the form of Fourier cosines series as follow

$$f(x)=\sum_{n=1}^{\infty}\left[\frac{2q_0}{\pi n}\left(\cos\frac{n\pi L_4}{L}-\cos\frac{n\pi L_1}{L}\right)\times\sin\left(\frac{n\pi x}{L}\right)\right] \qquad (5)$$

Approximate heat flux function, Eq. (5), is plotted with different values of n as shown in Fig. 3. At $n=100$, it is found that heat flux q is approximated to a constant value of q_0 at the evaporating part and condensing part.

The frictional force per unit volume of pipe F can be expressed in terms of a two-phase friction factor f as follows

$$F=\frac{4}{d}\tau_w=\frac{4}{d}\left[f\left(\frac{\rho u^2}{2}\right)\right]=\frac{2}{\rho d}G^2 f \qquad (6)$$

Subject to assumption (2) above, using the homogeneous model it is necessary to apply suitably defined single-phase friction factor to two-phase flow. The two-phase friction factor

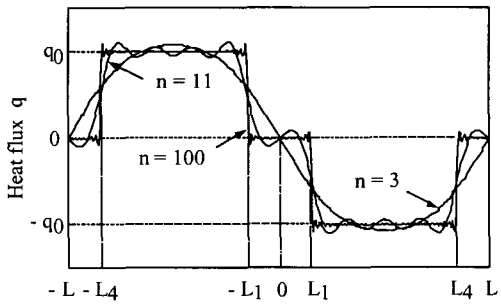

Fig. 3 Approximation of heat flux distribution.

f has been evaluated using a mean two-phase viscosity μ in the normal friction factor relationships with assuming that the friction factor may be expressed in terms of the Reynolds number by the Blasius equation.[11]

$$f = 0.079\left(\frac{Gd}{\mu}\right)^{-1/4} \tag{7}$$

where,

$$\frac{1}{\mu} = \frac{X}{\mu_g} + \frac{1-X}{\mu_f} \tag{8}$$

The pressure gradient is proportional to mass flow rate, $\dot{m}$, was introduced by Miyazaki et al.,[12] as follows:

$$-\frac{\partial p}{\partial x} = \dot{m}\frac{128\upsilon}{\pi d^4} = \frac{32\upsilon}{d^2}G \tag{9}$$

The homogeneous fluid density ρ, specific volume v and specific enthalpy h can be expressed in the quality X of mixed flow as follows.

$$\rho = \rho_f + X(\rho_g - \rho_f) = \rho_f + X\rho_{fg} \tag{10}$$

$$v = v_f + X(v_g - v_f) = v_f + Xv_{fg} \tag{11}$$

$$h = h_f + X(h_g - h_f) = h_f + Xh_{fg} \tag{12}$$

Substituting Eqs. (3)~(12) into Eqs. (1)~(2), and rearranging, the momentum and energy equations are changed to the following general equations.

$$\frac{\partial G}{\partial t} + G^2 v_{fg}\frac{\partial X}{\partial x} = \frac{32\upsilon}{d^2}G - \frac{2}{\rho d}G^2 f - (\rho_f + X\rho_{fg})g \tag{13}$$

$$\frac{\partial X}{\partial t} + (v_f + Xv_{fg})G\frac{\partial X}{\partial x} = -(v_f + Xv_{fg})\frac{8q_0}{dh_{fg}} \times \sum_{n=1}^{100}\left[\frac{1}{\pi n}\left(\cos\frac{n\pi L_4}{L} - \cos\frac{n\pi L_1}{L}\right)\sin\frac{n\pi x}{L}\right] \tag{14}$$

where the vapor quality, X, is correlated with the charging ratio, α, through the model proposed by Abdul-Razzak et al.[13] It can be expressed in the following form using the Martinelli parameter, X_{tt}

$$\alpha = \frac{1}{1 + 0.49X_{tt}^{0.803}} \tag{15}$$

where

$$X_{tt} = \left(\frac{1-X}{X}\right)^{0.9}\left(\frac{\rho_g}{\rho_f}\right)^{0.5}\left(\frac{\mu_f}{\mu_g}\right)^{0.1} \tag{16}$$

The initial condition, $\alpha = \alpha_0$, $X = X_0$.

In the above equations, it is found that they are nonlinear partial differential equations, which decide the variations of G and X. The numerical analysis is conducted and G & X can be solved.

4. Discussions

For conducting numerical analysis and flow visualization experiments, R-142b is chosen as the working fluid. The parameters used in the numerical modeling are listed in Table 1.

When the charging ratio of the working fluid was 40 vol.%, the variations of the theoretically predicted mass velocity G with respect to time according to the given heat fluxes are shown in Fig. 4. Figure 4 (a) shows the oscillation of the mass velocity G at the heat flux of 0.5 W/cm^2. The oscillation of the mass velocity was un-

Table 1 Experimental parameters

Parameters	Values	Parameters	Values
D [mm]	1.5, 3	α_0 [Vol.%]	20, 40, 80
ρ_f [kg/m^3]	1097	ρ_g [kg/m^3]	17.721
v_f [m^3/kg]	0.912e−3	v_g [m^3/kg]	56.43e−3
h_f [J/kg]	233280	h_g [J/kg]	429960
υ_f [m^2/s]	0.256e−6	υ_g [m^2/s]	0.603e−6
L [m]	0.220	q_0 [W/cm^2]	0.5, 1, 2

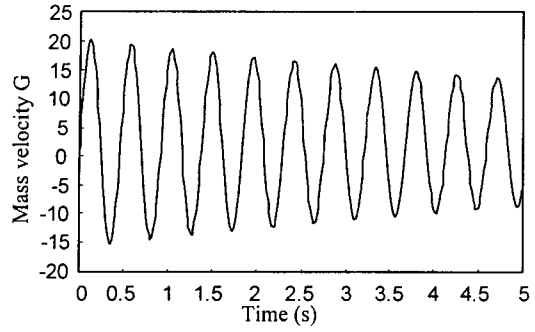

(a) q=0.5 (W/cm^2), α=40 (vol.%)

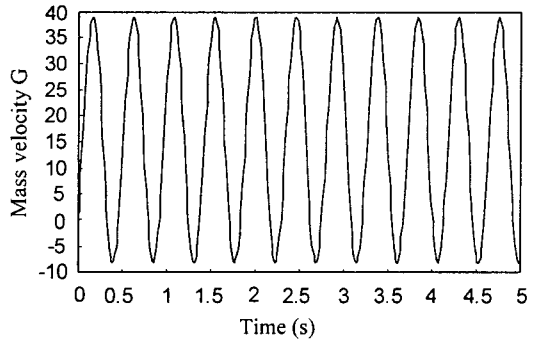

(b) q=1 (W/cm^2), α=40 (vol.%)

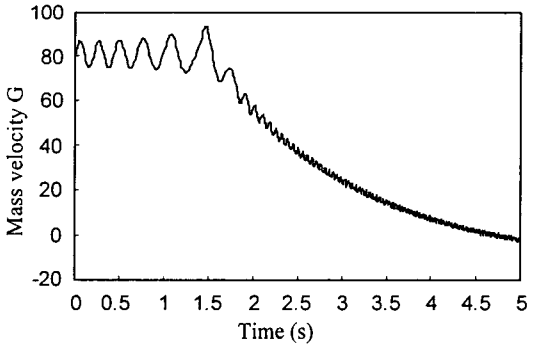

(c) q=2 (W/cm^2), α=40 (vol.%)

Fig. 4 Mass velocity according to the given heat fluxes.

steady due to the decrease of amplitude oscillation. This phenomenon was observed through the flow visualization experiments and is explained as follows: At the heat flux of 0.5 W/cm^2, the generation and the growth of bubbles in the OCHP were a nucleate boiling process at some turns among total flow channels. The bubbles grew and coalesced to become vapor plugs, and the oscillation phenomenon in that turns occurred. At the remaining turns of total flow channels, bubbles were intermittently generated, and the oscillation phenomenon was not clearly confirmed. Because of the inter-connection of the channels, the oscillation of mass velocity in the total flow channels decreased.

When the heat flux was increased to 0.9 W/cm^2, the oscillation of the vapor plugs and liquid slugs occurred very actively in each flow channel. The steady operating state of the OCHP was obtained. The theoretical prediction of mass velocity presented in Fig. 4 (b) shows that the oscillation of the mass velocity is steady at the heat flux condition of 1 W/cm^2. It can be seen that there is an agreement between the numerical predicted results and the experimental results. This steady state of the OCHP were also observed through the flow visualization experiments in the works of Kim et al.,[14] and Lee et al.[15]

However, as the heat flux was continuously increased, the working fluid supplied to the evaporating part was not sufficient. The dry-out phenomena occurred and the oscillation of the vapor plugs and liquid slugs became slow. This was due to the fact that some of flow channels in the evaporating part started to be filled with vapor. The supply of working fluid to the evaporating part reduced. This led to an increase in the surface temperature of the channels in the evaporating part. The liquid condensed in the condensing part was evaporated at the superheated tube wall before arriving normally in the evaporating part. Only the vapor phase existed in the evaporating part. Hence, the oscillation phenomenon gradually reduced and finally stopped. This state was theoretically predicted and shown in Fig. 4 (c). The oscillation of the mass velocity G decreased to zero when the heat flux was increased to q=2 W/cm^2.

At the heat flux condition of 1 W/cm^2, the variations of the theoretically predicted mass velocity G with respect to time according to

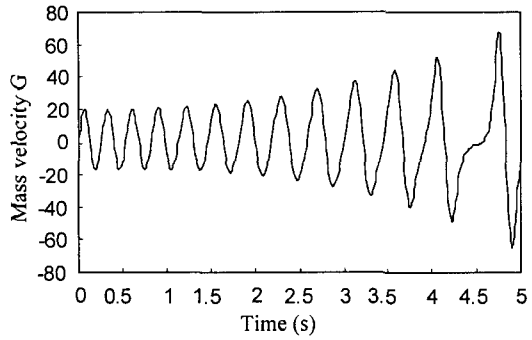

(a) α=80 (vol.%), q=1 (W/cm^2)

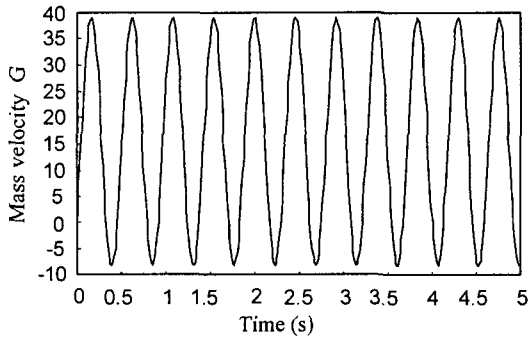

(b) α=40 (vol.%), q=1 (W/cm^2)

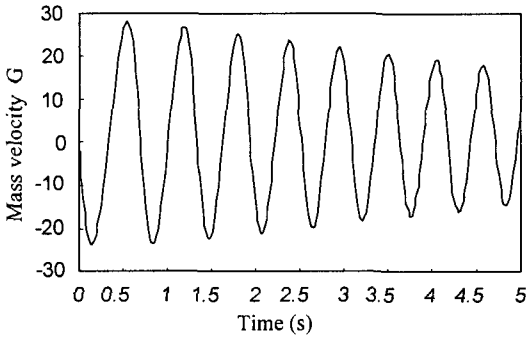

(c) α=20 (vol.%), q=1 (W/cm^2)

Fig. 5 Mass velocity according to the different charging ratios of working fluid.

the different charging ratios of working fluid are shown in Fig. 5. The oscillation of the mass velocity G was almost symmetric at the charging ratio of 80 vol.% as shown in Fig. 5 (a). However, the oscillation of the mass velocity was unsteady due to the increase of oscillation amplitude and the decrease of frequency. The experimental observations on this state showed that the excessive charge of the working fluid led to the increase of saturation pressure in the OCHP. This increased the temperature difference and the pressure difference between the evaporating part and the condensing part. The operating state of the OCHP changed to an unsteady state.[15]

Figure 5 (b) showed the oscillation of the mass velocity G at the charging ratio of 40 vol.%. The oscillation of the mass velocity was steady. This state can be the optimal operation state of the OCHP predicted by theoretical model. Active oscillations of working fluid were also observed at charging ratio of 40 vol.% through the flow visualization experiments. With this charging ratio, the circulation velocity was at maximum value, which results in best heat transfer performance. The oscillation of vapor plugs and liquid slugs occurred very actively between the evaporating part and the condensing part. It was observed that a thin liquid film was formed on the walls of the channels. The liquid film decreased the thermal resistance between the surface of the walls and the working fluid because a pseudo slug flow pattern near the annular flow pattern was confirmed by the very rapid oscillation of the vapor plugs and liquid slugs along the flow channels. Besides, the bubbles formed within the thin liquid film in the evaporating part separated shortly after they generated from the heated walls. The space vacated by the separated bubbles was filled by the liquid in the liquid film and the nucleate boiling process continuously occurred. Consequently, the heat transfer coefficient of nucleate boiling increased. It can be seen that the present numerical results agreed well to the experimental results for this operation state of the OCHP.

Figure 5 (c) showed the oscillation of the mass velocity G at the charging ratio of 20 vol.%. The oscillation was unsteady due to the decrease of oscillation amplitude. This state was observed through the flow visualization experi-

ments and was explained as follows: At the charging ratio of 20 vol.%. The temperature difference and the pressure difference between the evaporating part and the condensing part decreased due to the lack of the liquid in the OCHP. The working fluid supplied to the evaporating part was not sufficient. The evaporation occurred on the superheated walls in the evaporating part and the local dry-out phenomena occurred in some flow channels. Hence the oscillation phenomenon was low and unsteady.

The oscillating motion of working fluid in the OCHP is affected by the cross section geometry of flow channel. When the charging ratio of the working fluid was 40 vol.% and the heat flux was 1 W/cm^2, the variations of the theoretically predicted mass velocity G with respect to time according to the different hydraulic diameters are shown in Fig. 6. In the case of 1.5 mm diameter, the oscillation was steady. When the diameter was increased to d=3 mm, the oscillation amplitude decreased. From flow visualization experiments, it can explain that the capillary force is not dominant over the gravitation force in a large diameter tube. During the initial period, at the moment after working fluid was partially filled in OCHP, the generation of vapor-liquid slug-train units by capillary force reduced in the large diameter tube. Consequently, the oscillation of working fluid decreased when heat was applied to the evaporating part of OCHP.

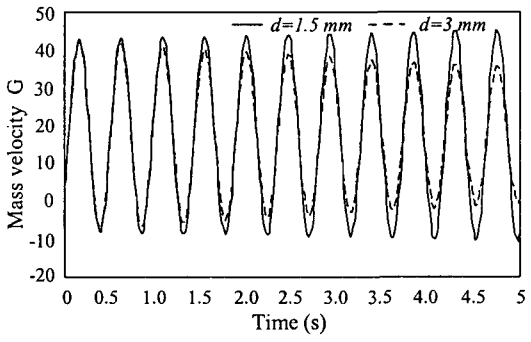

Fig. 6 Mass velocity according to the different hydraulic diameters.

5. Conclusion

A theoretical model of the OCHP was developed to model the oscillating motion of working fluid in the OCHP. The mass velocity inside of the OCHP was solved based on the theoretical model and differential equations of two-phase flows. From the analysis of the numerical results, it was found that the oscillating motion of working fluid in the OCHP was affected by the operation and design conditions such as the heat flux, the charging ratio of working fluid and the hydraulic diameter of flow channel. The proposed model could be used for estimating the oscillating motion of working fluid in the OCHP. Further experimental investigations are needed to verify the performance improvements and the theoretical model.

Acknowledgements

The authors wish to acknowledge the partially financial support of the Brain Korea 21 Project in 2003.

References

1. Akachi, H., 1994, Loop type serpentine capillary tube heat pipe, Proceedings of 71th General Meeting Conference of JSME, Vol. 3, No. 940-10, pp. 606-611.
2. Akachi, H., Polasek, F. and Stulc, P., 1996, Pulsating heat pipes, Proceedings of 5th Int. Heat Pipe Symposium, Melbourne, pp. 208-217.
3. Kim, J. S., Lee, W. H., Lee, J. H., Jung, H. S., Kim, J. H. and Jang, I. S., 1999, Flow visualization of oscillating capillary tube heat pipe, Proceeding of Thermal Engineering Conference of KSME, pp. 65-70.

4. Lee, W. H., Jung, H. S., Kim, J. H. and Kim, J. S., 1999, Flow visualization of oscillating capillary tube heat pipe, 11th International Heat Pipe Conference, Tokyo, Japan, Vol. 2, pp. 131-136.
5. Miyazaki, Y. and Arikawa, M., 1999, Oscillatory flow in the oscillating heat pipe, 11th International Heat Pipe Conference, Tokyo, Japan, Vol. 2, pp. 143-148.
6. Dobson, R. T. and Hams, T. M., 1999, Lumped parameter analysis of closed and open oscillatory heat pipe, 11th International Heat Pipe Conference, Tokyo, Japan, Vol. 2, pp. 137-142.
7. Wong, T. N., Tong, B. Y., Lim, S. M. and Ooi, K. T., 1999, Theoretical modeling of pulsating heat pipe, 11th International Heat Pipe Conference, Tokyo, Japan, Vol. 2, pp. 159-163.
8. Maezawa, S., Nakajima, R., Minamisawa, A. and Gi, K., 1996, Basic study on oscillating capillary tube thermosyphon, 33th National Heat Transfer Symposium of Japan, pp. 197-198.
9. Maezawa, S., Izumi, T., Nakazima, R. and Gi, K., 1997, Nonliner chaotic characteristics of oscillating heat pipe, 34th National Heat Transfer Symposium of Japan, Vol. 1, pp. 275-276.
10. Maezawa, S., Sato, F. and Gi, K., 2000, Chaotic dynamics of looped oscillating heat pipes, Proceedings of the 6th International Heat Pipe Symposium, Chiang Mai, Thailand, pp. 404-412.
11. John, G. C. and John, R. T., 1994, Convective Boiling and Condensation, Clarendon Press, Oxford Third edition, pp. 44-45.
12. Miyazaki, Y. and Akachi, H., 1998, Self-excited oscillation of slug flow in a micro channel, Third International Conference on Multiphase Flow, Lyon, France, pp. 1-5.
13. Abdul-Razzak, A., Shoukri, M. and Chang, J. S., 1995, Characteristics of refrigerant R134a liquid-vapor two-phase flow in horizontal pipe, ASHRAE Transactions Symposium, pp. 953-964.
14. Kim, J. S., Jung, H. S., Kim, J. H. and Kim, J. W., 2001, Flow visualization of oscillation characteristics of liquid and vapor in oscillating capillary tube heat pipe, The 6th Asian Symposium on Visualization, Pusan, Korea, pp. 398-401.
15. Lee, W. H., Kim, J. H., Kim, J. S. and Jang, I. S., 1999a, The heat transfer characteristics of oscillating capillary tube heat pipe, 2nd Two-Phase Flow Modelling and Experimentation, Pisa, Italy, Vol. 3, pp. 1713-1718.